CrystEngComm

Accepted Manuscript

ROYAL SOCIETY OF CHEMISTRY

www.rsc.org/crystengcomm

CrystEngComm RSCPublishing

ARTICLE

Mechanochemical synthesis and characterisation of two new bismuth metal organic frameworks†

Cite this: DOI: 10.1039/x0xx00000x

L. Tröbs,[a] M. Wilke,[a] W. Szczerba,[a] U. Reinholz,[a] and F. Emmerling[a*]

Received 00th January 2012,
Accepted 00th January 2012

DOI: 10.1039/x0xx00000x

www.rsc.org/

Two metal organic structures composed of the ligands benzene-1,4-dicarboxylate and pyridine-2,5-dicarboxylate and bismuth cations are presented: $(H_2Im)[Bi(1,4\text{-}bdc)_2]$ **(1)** and $[Bi(pydc)(NO_3)_2(H_2O)_2]*H_2O$ **(2)** (bdc = benzenedicarboxylate, H_2Im = imidazole cation, pydc = pyridinedicarboxylate). Both compounds were synthesised via grinding and the crystal structure of compound **(2)** was solved based on its powder diffraction pattern. Compound **1** crystallises isostructurally to the dimethyl ammonium containing compound $(dma)[(Bi(1,4\text{-}bdc)_2]$. Raman spectroscopy and Extended X-ray absorption fine structure (EXAFS) measurements provided additional information about the two mechanochemically synthesised metal organic compounds.

Introduction

The synthesis and thorough characterisation of novel metal organic compounds and metal organic frameworks (MOFs) are of considerable scientific interest due to their manifold properties.[1-4] Possible applications of these compounds range from gas storage, gas separation to drug-carrier, magnetism, and catalysis.[4-8] Metal organic compounds consist of different tuneable molecular structures and have accordingly a large variety of possible architectures and topologies. Typically, transition metals are employed as metal centres in MOFs, whereas examples including main group metals are scarce.[9-11] In this context, MOFs containing bismuth as metal centres are currently investigated in greater detail.[12] Connected via organic ligands, bismuth cations offer a wide range of structural diversity. Bi^{3+} cations are known for their stereo active lone pair leading to interesting and versatile coordination geometries.[13] Moreover, bismuth shows low toxicity even though its position in the periodic table suggests contrary findings. The pharmaceutical value of bismuth and its complexes is well documented, e.g. bismuth subsalicylate complexes have been used successfully in the treatment against gastritis and similar stomach diseases.[14, 15]
Dicarboxylate ligands are widely used to link metal centres in metal organic frameworks. In combination with Bi^{3+} cations as inorganic metal centres the structural diversity is even higher. Recently, a number of metal organic compounds including bismuth centres and dicarboxylate ligands have been reported.[12, 16-21] Small changes in the synthesis of these compounds can lead to different crystalline structures. Thirumurugan *et al*. reported four different MOF structures including Bi^{3+} cations and benzene-1,4-dicarboxylate synthesised by changing the metal precursor or the reducing agent.[12] Recently, Wibowo *et al*. presented a solvothemal and hydrothermal synthesis for three different bismuth - pyridine-2,5-dicarboxylate structures by varying the applied base from potassium hydroxide to sodium hydroxide.[16] These syntheses require a certain amount of solvents and reaction times up to several days. Here, mechanochemical syntheses are an efficient and fast alternative.[22-27] Mechanochemistry prevents the use of large amounts of solvents and proceeds at ambient temperatures. Typically, pure products are obtained in high yields within minutes.
In the present work, two metal organic compounds containing Bi^{3+} cations as metal centres and benzene-1,4-dicarboxylate ($(H_2Im)[Bi(1,4\text{-}bdc)_2]$ **(1)**) or pyridine-2,5-dicarboxylate ($[Bi(pydc)(NO_3)_2(H_2O)_2]*H_2O$ **(2)**) as ligands are presented. Both compounds were synthesised mechanochemically. Compound **(1)** is the solvent free analogue to the dma containing MOF reported by Thirumurugan *et al.* The crystal structure of **(2)** was solved and refined from powder diffraction data. The characterisation of the crystal structures is backed by Raman spectroscopy and EXAFS measurements.

Results and discussion

Two metal carboxylates including Bi^{3+} cations and benzene-1,4-dicarboxylate ($(H_2Im)[Bi(1,4\text{-}bdc)_2]$ **(1)**) or pyridine-2,5-dicarboxylate ($[Bi(pydc)(NO_3)_2(H_2O)_2]*H_2O$ **(2)**) have been synthesised mechanochemically. For both syntheses Bismuth(III) nitrate pentahydrate was used as precursor. Compound **(1)** was synthesised by grinding Bismuth(III) nitrate pentahydrate together with the ligand benzene-1,4-dicarboxylic acid and imidazole as proton acceptor in the ratio 1:2:4 (Scheme 1). Under mechanochemical conditions, bismuth nitrate decomposes and HNO_3 evaporates from the reaction mixture after opening the grinding jar. The completeness of the reaction was confirmed by powder X-ray diffraction measurements (Figure 1, top). A comparison with database entries revealed a good agreement of the XRD pattern of **(1)** with the diffraction pattern of $(dma)[(Bi(1,4\text{-}bdc)_2]$ (dma = dimethyl ammonium cation) (Figure 1, top).[12] It is reasonable, that protonated imidazole cations replace the dma

cations in the structure obtained under mechanochemical conditions leading to an isotypic structure.

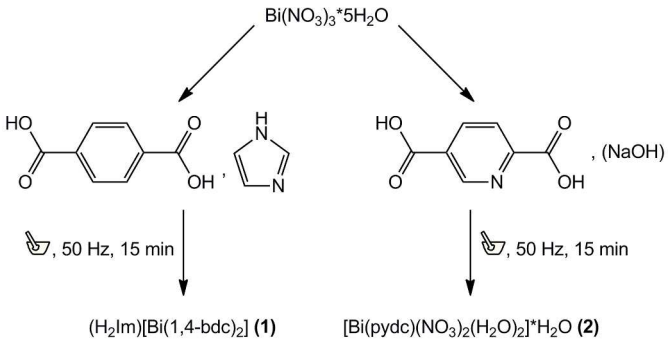

Scheme 1: Reaction scheme of the syntheses of (H_2Im)**[**$Bi(1,4\text{-}bdc)_2$**]** **(1)** (left) and $[Bi(pydc)(NO_3)_2(H_2O)_2]*H_2O$ **(2)** (right).

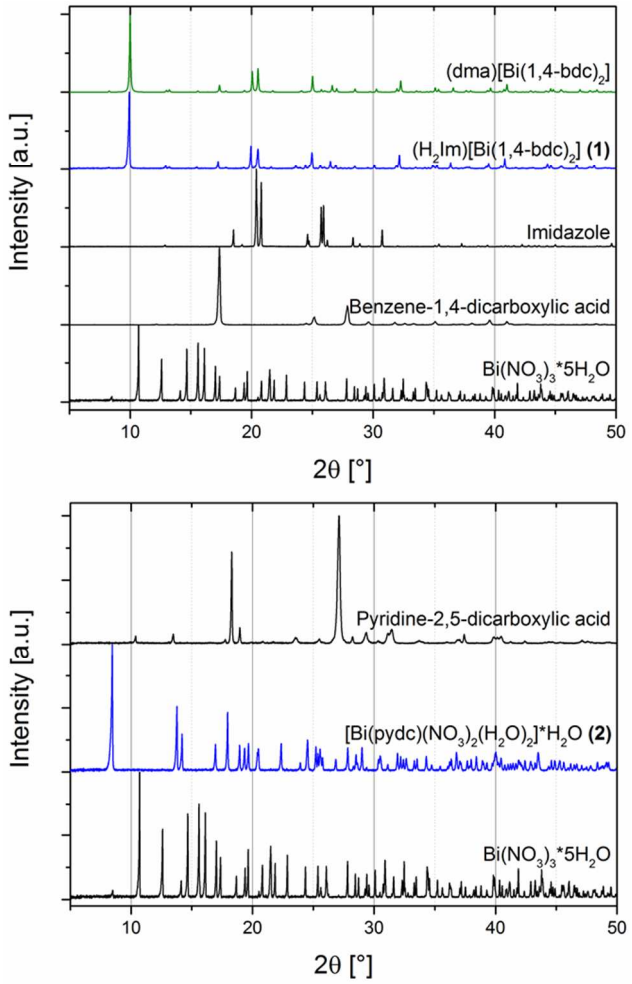

Figure 1: Top: Powder XRD patterns of the metal organic compound (H_2Im)**[**$Bi(1,4\text{-}bdc)_2$**]** **(1)** (blue), starting materials (black) Bismuth(III) nitrate pentahydrate $(Bi(NO_3)_3*5H_2O)$, benzene-1,4-dicarboxylic acid, and imidazole and powder XRD pattern for comparison of (dma)$[Bi(1,4\text{-}bdc)_2]$ (green) simulated based on its crystal structure (CCDC 776715, CSD-XAFBOX).[12]
Bottom: Powder XRD patterns of the synthesised metal organic structure $[Bi(pydc)(NO_3)_2(H_2O)_2]*H_2O$ **(2)** (blue) and starting materials (black) Bismuth(III) nitrate pentahydrate $(Bi(NO_3)_3*5H_2O)$ and pyridine-2,5-dicarboxylic acid.

For the synthesis of compound **(2)** Bismuth(III) nitrate pentahydrate, pyridine-2,5-dicarboxylic acid and a small amount of a sodium hydroxide solution (200 µL, 1 M) were ground together for 15 minutes. Sodium hydroxide acts as reducing agent during the reaction.
The comparison of the powder diffraction patterns of Bismuth(III) nitrate pentahydrate, pyridine-2,5-dicarboxylate and the product **(2)** indicates the completeness of the reaction (see, Figure 1, bottom). The diffraction pattern of **(2)** could not be assigned to any database entry. The structure was solved from the powder diffraction pattern leading to the first description of the compound $[Bi(pydc)(NO_3)_2(H_2O)_2]*H_2O$.

Structure of $(H_2Im)[Bi(1,4\text{-}bdc)_2]$ (1)

The mechanochemical synthesised three-dimensional metal organic framework $(H_2Im)[Bi(1,4\text{-}bdc)_2]$ **(1)** crystallises in the rhombohedral spacegroup *R*-3*c*. The crystal data of this structure are summarised in Table 1. The asymmetric unit cell consists of two different Bi^{3+} cations, one benzene-1,4-dicarboxylate anion, and one imidazole cation. The two Bi^{3+} cations Bi1 and Bi2 are present in the ratio of 1(Bi1) to 2(Bi2). Both are holodirected with a stereochemically inactive lone pair. Bi1 is twelve-coordinated and Bi2 is nine-coordinated by six different benzene-1,4-dicarboxylate molecules, respectively. The connection between the benzene-1,4-dicarboxylate molecules and the bismuth polyhedra results in a three-dimensional framework (Figure 2).[1, 3, 12]

Table 1: Crystal data and structure refinement parameters for (H_2Im)**[**$Bi(1,4\text{-}bdc)_2$**]** **(1)**[12] and $[Bi(pydc)(NO_3)_2(H_2O)_2]*H_2O$ **(2)**.

Structure parameter	$(H_2Im)[Bi(1,4\text{-}bdc)_2]$ **(1)**	$[Bi(pydc)(NO_3)_2(H_2O)_2]*H_2O$ **(2)**
Empirical formula	$C_{19}H_{13}N_2O_8Bi$	$C_7H_9N_3O_{13}Bi$
Formula weight ($g mol^{-1}$)	606.30	552.14
Crystal system	Rhombohedral	Triclinic
Space group	*R*-3*c*	*P*1
a (Å)	17.6932(7)	5.10416(9)
b (Å)	17.6932(7)	6.8558(3)
c (Å)	29.7350(9)	10.8069(2)
α (°)	90	104.328(1)
β (°)	90	90.119(1)
γ (°)	120	104.302(1)
V ($Å^3$)	8061.42(68)	354.23(1)
Z	18	1
D_{calc} ($g cm^{-3}$)	2.163	2.557
R_{wp}		10.4
R_{Bragg}		5.156
GOF		1.64

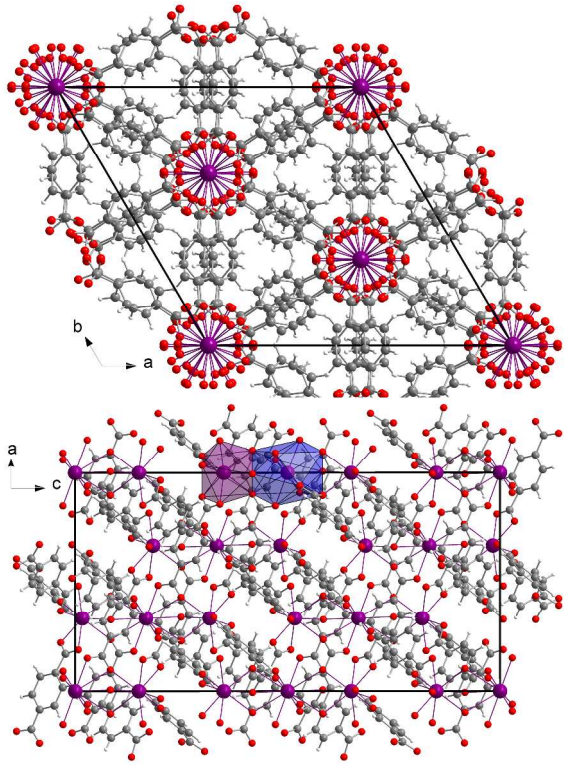

Figure 2: View of the three-dimensional structure $(H_2Im)[Bi(1,4\text{-}bdc)_2]$ **(1)** seen along the *c*-axis (top) and the *b*-axis (bottom). The coordination polyhedra of both Bi^{3+} cations are given in blue (Bi1, twelve-coordinated) and violet (Bi2, nine-coordinated) in the view of the *a*-*c* plane (bottom).

EXAFS measurements at the Bi L_3-edge were performed for compound **(1)**. These measurements provide information about the coordination environment of the Bi^{3+} cations. EXAFS data for structure **(1)** shown in real space are given in Figure 3, left and the according fit parameters are summarized in Table 2. The fitted comparison data were calculated based on the crystal structure. For the evaluation single-scattering paths of the first coordination shell of the Bi centres were used. A good agreement of the experimental data to the fit results could be proven. The root mean square error (RMSE) of the atom distances for structure $(H_2Im)[Bi(1,4\text{-}bdc)_2]$ **(1)** is 0.145 Å. This proves a good agreement of the theoretical atom distances to the experimentally received distances. Thus, the crystal structure and especially the coordination spheres of the two Bi^{3+} cations could be proven by EXAFS measurements.

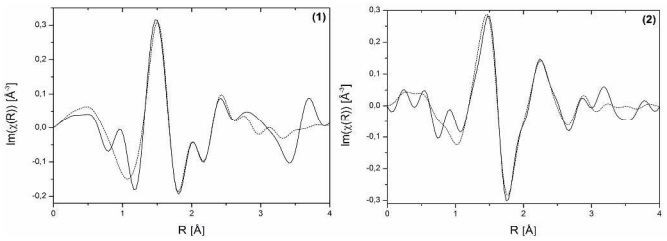

Figure 3: Bi L_3-edge EXAFS data shown in real space for (H_2Im)**[**$Bi(1,4\text{-}bdc)_2$**]** **(1)** and $[Bi(pydc)(NO_3)_2(H_2O)_2]*H_2O$ **(2)**. Experimental data - solid line, fit results - dotted line.

Table 2: EXAFS fit parameters of (H_2Im)**[**$Bi(1,4\text{-}bdc)_2$**]** **(1)** and $[Bi(pydc)(NO_3)_2(H_2O)_2]*H_2O$ **(2)**. Root mean square error (RMSE) for $(H_2Im)[Bi(1,4\text{-}bdc)_2]$ **(1)** is 0.145 Å and for $[Bi(pydc)(NO_3)_2(H_2O)_2]*H_2O$ **(2)** 0.249 Å.

Sample	Scattering path	R_{model} [Å]	R_{fit} [Å]	$R_{diff}{}^2$ [Å^2]
(1)	Bi1-O1	2.49	2.35	0.0169
	Bi1-O2	3.04	3.10	0.0036
	Bi1-C1	3.13	3.37	0.0576
	Bi2-O3	2.31	2.21	0.0081
	Bi2-O4	2.61	2.54	0.0036
	Bi2-O2	2.67	2.75	0.0049
	Bi2-C8	2.81	3.04	0.0529
(2)	Bi1-O6	2.34	2.26	0.0064
	Bi1-O10	2.53	2.26	0.0729
	Bi1-N6	2.53	2.13	0.1681
	Bi1-O13	2.57	2.36	0.0441
	Bi1-O5	2.59	2.49	0.0100
	Bi1-O2	2.65	2.57	0.0064
	Bi1-O2	2.71	2.87	0.0256
	Bi1-O11	2.79	3.10	0.0961
	Bi1-O8	2.80	2.77	0.0009
	Bi1-N2	2.96	3.02	0.0036
	Bi1-O1	3.11	3.32	0.0441
	Bi1-N1	3.17	3.49	0.0961
	Bi1-N1	3.20	3.63	0.1849
	Bi1-C3	3.24	3.17	0.0064
	Bi1-C5	3.34	3.65	0.0961
	Bi1-C1	3.47	3.83	0.1296

Structure of $[Bi(pydc)(NO_3)_2(H_2O)_2]*H_2O$ (2)

The crystal structure of $[Bi(pydc)(NO_3)_2(H_2O)_2]*H_2O$ **(2)** was calculated based on its powder diffraction data. Figure 4 shows the result of the Rietveld refinement illustrating the good agreement of the simulated powder pattern with the measured one. The refinement converged at an R_{wp} = 10.4%. The crystal data are given in Table 1. $[Bi(pydc)(NO_3)_2(H_2O)_2]*H_2O$ **(2)** crystallises in the triclinic space group, *P*1, Z = 1, with unit cell parameters of a = 5.10416(9) Å, b = 6.8558(3) Å, c = 10.8069(2) Å, α = 104.328(1)°, β = 90.119(1)°, γ = 104.302(1)°, and V = 354.23(1) Å^3. The asymmetric unit cell contains one Bi^{3+} cation, one pyridine-2,5-dicarboxylate anion, two nitrate anions and three water molecules. The Bi^{3+} cation is nine-coordinated and holodirected with a stereochemically inactive lone pair of electrons. The Bi^{3+} cation coordinates bidentate to the nitrogen atom and one carboxylate oxygen atom of the pyridine-2,5-dicarboxylate molecule. The coordination environment is completed by two water molecules, two nitrate units coordinating bidentate, and a third nitrate anion coordinating monodentate. In addition, one uncoordinated water molecule is near the second carboxylate unit of the pyridine-2,5-dicarboxylate. The Bi-N bond length amounts to 2.533 Å and the Bi-O bond lengths are in the range of 2.337 - 2.798 Å. The monodentate coordinated nitrate anion connects this complex to adjacent Bi^{3+} cations. Consequently, a one-dimensional chain of nine-coordinated Bi^{3+} cations is formed (Figure 5). The chains are arranged parallel to each other running along the *a*-axis.

The coordination sphere around the Bi^{3+} cation and thereby the crystal structure of compound **(2)** could be backed by EXAFS measurements conducted at the Bi L_3-edge. EXAFS data shown in real space and the fit parameters are given in Figure 4, right and Table 2. The fitted comparison data, based on the crystal structure from the powder diffraction pattern, showed a good agreement to the experimental data. The first scattering path was used for evaluation. The RMSE of the atom distances for structure ($[Bi(pydc)(NO_3)_2(H_2O)_2]*H_2O$ **(2)** is 0.249 Å. This proves a good agreement of the calculated atom distances to the experimentally received distances.

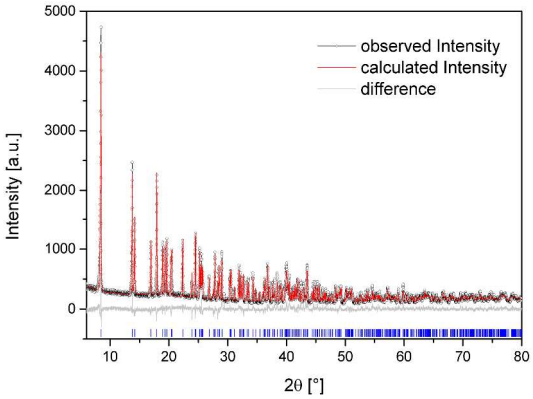

Figure 4: Scattered X-ray intensity for structure **(2)** at ambient conditions as a function of diffraction angle 2θ. The observed pattern (circles), the best Rietveld fit profile (red line), the reflection positions (blue tick marks), and the difference curve (grey line) between observed and calculated profiles are shown. The wavelength was $\lambda = 1.54056$ Å ($CuK_{\alpha 1}$). The R-values are $R_p = 8.0\%$, $R_{wp} = 10.4\%$; R_p, and R_{wp} refer to the Rietveld criteria of fit for profile, weighted profile, and structure factor, defined by Langford and Louer.[28]

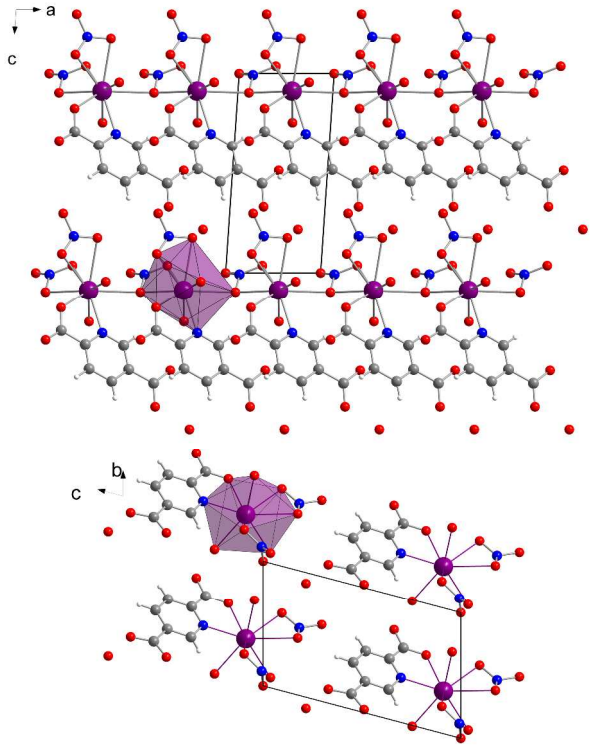

Figure 5: View of the chain structure $[Bi(pydc)(NO_3)_2(H_2O)_2]*H_2O$ **(2)** along the *b*-axis (top). Representation of the packing of the molecules in a projection along the *a*-axis. (bottom). For each projection the polyhedron around one Bi^{3+} cation is shown in violet. The hydrogen atoms of the water molecules were omitted for clarity.

Like other bismuth carboxylates described in the literature, compound **(1)** and **(2)** show the ability of bismuth to adopt a high coordination environment, typical coordination numbers are eight or nine.[29-32] The Bi–O distances in these structures range between 2.21 to 3.13 Å. Raman spectra for both structures $(H_2Im)[Bi(1,4\text{-}bdc)_2]$ **(1)** and $[Bi(pydc)(NO_3)_2(H_2O)_2]*H_2O$ **(2)** as well as for the starting materials are shown in Figure 6. The compounds **(1)** and **(2)** show characteristic Raman bands and comparison to the Raman spectra of the respective starting materials Bismuth(III) nitrate pentahydrate, pyridine-2,5-dicarboxylic acid, benzene-1,4-dicarboxylic acid and imidazole proves the completeness of the reaction. Both structures **(1)** and **(2)** show few similar Raman bands to the ligands benzene-1,4-dicarboxylic acid and pyridine-2,5-dicarboxylic acid but they are clearly shifted in the products due to deprotonation and new coordination spheres of the ligands in the final products. For the synthesis of compound **(1)** the protonation of the added imidazole molecule can be verified based on the Raman spectra. Two intensive bands at 1220 cm^{-1} and 1445 cm^{-1} characterize the spectrum of the imidazolium ion (H_2Im).[33] These bands are clearly detectable in the Raman spectrum of compound **(1)**.

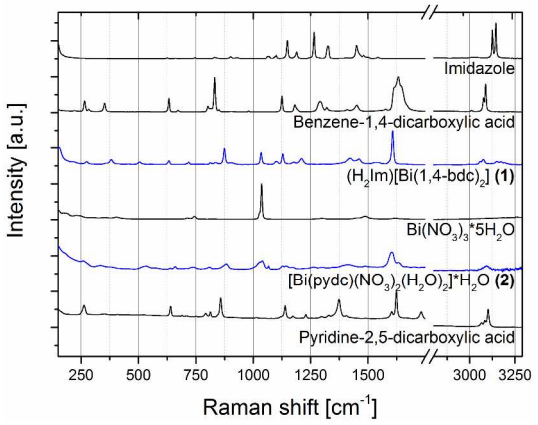

Figure 6: Raman spectra of the products (H_2Im)**[**$Bi(1,4\text{-}bdc)_2$**]** **(1)** and $[Bi(pydc)(NO_3)_2(H_2O)_2]*H_2O$ **(2)** (blue) in comparison with the Raman spectra of the starting materials pyridine-2,5-dicarboxylic acid, Bismuth(III) nitrate pentahydrate ($Bi(NO_3)_3*5H_2O$), benzene-1,4-dicarboxylic acid and imidazole (black).

Experimental

Materials

Bismuth(III) nitrate pentahydrate $Bi(NO_3)_3*5H_2O$ (98%, Alfa Aesar, Karlsruhe, Germany), benzene-1,4-dicarboxylic acid (terephthalic acid) $C_6H_4(COOH)_2$ (98+%, Alfa Aesar, Karlsruhe, Germany), imidazole $C_3H_4N_2$ (99%, Alfa Aesar, Karlsruhe, Germany) and pyridine-2,5-dicarboxylic acid $C_5NH_3(COOH)_2$ (for synthesis, Merck, Hohenbrunn, Germany) were used without further purification. A 1 M sodium hydroxide solution was prepared using solid sodium hydroxide (for analysis, Merck, Darmstadt, Germany) and MilliQ water (18.2 MΩ, ultrapure water system seralpur Pro 90 CN, Seral, Ransbach-Baumbach, Germany).

Sample preparation

$(H_2Im)[Bi(1,4\text{-}bdc)_2]$ (1). In a typical synthesis of **(1)** $Bi(NO_3)_3*5H_2O$ (590.0 mg, 1 e.q.), benzene-1,4-dicarboxylic acid (404.1 mg, 2 e.q.), and imidazole (331.2 mg, 4 e.q.) were ground together in a conventional ball mill (Pulverisette 23, FRITSCH GmbH, Idar-Oberstein, Germany) for 15 minutes with a frequency of 50 Hz. A 10 mL steel grinding bowl and two steel balls with 10 mm diameter were used. The product was obtained as white slurry and dried in air.

$[Bi(pydc)(NO_3)_2(H_2O)_2]*H_2O$ (2). For a typical synthesis of **(2)**, $Bi(NO_3)_3*5H_2O$ (723.9 mg, 1 e.q.) and pyridine-2,5-dicarboxylic acid (249.1 mg, 1 e.q.) were ground together with 200 µL of a NaOH solution (1 M) in a conventional ball mill (Pulverisette 23, FRITSCH GmbH, Idar-Oberstein, Germany) using a 10 mL steel grinding bowl and two steel balls (10 mm). The product was obtained as white-grey slurry and dried in air.

Methods

Powder diffraction measurements. Powder diffraction measurements were performed on a D8 Discover diffractometer (Bruker AXS, Karlsruhe, Germany) equipped with a Lynxeye detector and operated in transmission geometry (Cu-$K\alpha_1$ radiation, $\lambda = 0.154056$ nm). Samples were measured over a 2θ range of 5-80° with a step size of 0.009° and 0.5 to 2.5 s/step.

Structure determination. For the high resolution X-ray powder diffraction experiments, the sample was sealed in a glass capillary of 0.5 mm diameter (WJM-Glas, Müller GmbH, Berlin, Germany). Powder diffraction data were collected at room temperature. Indexing of the powder pattern of **(2)** using the indexing module of TOPAS[34] led to a primitive triclinic unit cell with lattice parameters given in Tab. 1. The number of formula units per unit cell could be determined to $Z = 1$ from packing considerations, indicating *P*1 as the most probable space group, which could later be confirmed by Rietveld refinement. The unit cell and space group were confirmed using CHEKCELL.[35] The structure determination of the structure $[Bi(pydc)(NO_3)_2(H_2O)_2]*H_2O$ **(2)** was carried out based on the powder XRD pattern. A structural starting model for Rietveld refinement was subsequently found with the Monte Carlo simulated annealing programme FOX.[36] This programme uses global-optimization algorithms to solve the structure by performing trials in direct space. This search algorithm uses random sampling coupled with simulated temperature annealing to locate the global minimum of the figure-of-merit factor. Parts of the molecule were refined as a rigid group to reduce the total number of degrees of freedom. Both nitrate molecules were set rigid, while pyridine-2,5-dicarboxylate was set rigid with the exception of the carboxyl oxygen and hydrogen atoms. In addition, a bond between the Bi atom and the nitrogen and one carboxyl oxygen atom of the pyridine-2,5-dicarboxylate was assigned. The crystal structure of $[Bi(pydc)(NO_3)_2(H_2O)_2]*H_2O$ **(2)** was solved by the simulated annealing procedure. The calculation process was carried out on a standard personal computer within 20 hours, finding the deepest minimum of the cost function several times during the procedure. The subsequent Rietveld refinement was performed using the TOPAS software.[34] The structural solution obtained from MC/SA was subsequently subjected to a Rietveld refinement. The refinement converged at an $R_{wp} = 10.4$ %. Selected bond lengths and angles of compound **(2)** are given in the Supporting Information (S - Table 1 and S - Table 2).

Raman spectroscopy. Raman spectra were collected using a Raman RXN1™ Analyzer (Kaiser Optical Systems, Inc., Ecully, France) with NIR excitation radiation at 785 nm. The spectrometer is equipped with a CCD camera (1024 × 256 pixels) and a non-contact probe head (working distance 15 mm, spot size 1 mm Ø). Raman spectra were recorded with an acquisition time of 5 × 5 s and an irradiance of 6.6 W/cm² on the sample.

EXAFS measurements. For the EXAFS measurements, both products were mixed with activated carbon and fixed in plastic sample holders. EXAFS measurements were performed at the electron storage ring BESSY II (Helmholtz-Zentrum Berlin für Materialien und Energie GmbH, Berlin, Germany) at the BAM*line*.[37, 38] The X-ray beam was monochromatised using a double-crystal monochromator (DCM). The size of the beam spot was 3 × 1 mm². The energy resolution of the setup was about 0.00015, leading to $\Delta E = 2.0$ eV while measuring at the Bi L_3 edge (13.419 keV). The excitation energy was varied from 13.250 to 14.271 keV in steps of 10 eV pre-edge, 1 eV at the edge and $\Delta k = 0.04$ in the k-space of the EXAFS region. Measurements were performed in transmission geometry. The first ionisation chamber was filled with argon (1 bar) and the second was filled with xenon (1 bar). The EXAFS data were evaluated using the programmes Athena, Artemis, and Hephaestus.[39] The model spectra for the fits were calculated using FEFF9 code.[40]

Elemental analysis. To exclude the presence of X-ray amorphous impurities elemental analyses were conducted. The results are in good agreement the expected values. Compound **(1)**: $BiC_{19}H_{13}O_8N_2$ (606.30 g mol^{-1}): calculated: C 37.64%, H 2.16%, N 4.62%; found: C 32.05%, H 3.10%, N 4.85%. For compound **(2)**: $BiC_7H_9N_3O_{13}$ (552.13 g mol^{-1}): calculated: C 15.23%, H 1.64%, N 7.61%; found: C 14.38%, H 1.73%, N 7.78%.

Conclusions

Two metal organic compounds containing bismuth and benzene-1,4-dicarboxylate or pyridine-2,5-dicarboxylate as ligand were synthesised mechanochemically. The crystal structure of compound **(1)** was identified based on its powder diffraction data. The crystal structure of the bismuth and pyridine-2,5-dicarboxylate containing compound **(2)** could be calculated from its powder diffraction pattern. The mechanochemical synthesis pathway revealed a fast, efficient, and solvent free access to both compounds. For both structures Raman spectra and EXAFS measurements revealed a good agreement of the calculated crystalline structures and the bismuth coordination spheres.

Notes and references

[a] BAM Federal Institute for Materials Research and Testing, Richard-Willstätter-Str. 11, 12489 Berlin, Germany

* corresponding author: Franziska Emmerling, BAM Federal Institute for Materials Research and Testing, Richard-Willstätter-Str. 11, 12489 Berlin, Germany, phone +49-30-8104-1133, fax +49-30-8104-1139, franziska.emmerling@bam.de

†CSD-978120 contains the supplementary crystallographic data for $[Bi(pydc)(NO_3)_2(H_2O)_2]*H_2O$ **(2)**. The data can be obtained free of charge from the Cambridge Crystallographic Data Centre via www.cdc.cam.ac.uk/data_request/cif.

1. S. Bauer and N. Stock, *Chem. Unserer Zeit*, 2008, **42**, 12-19.
2. G. Ferey, *Chem. Soc. Rev.*, 2008, **37**, 191-214.
3. J. L. C. Rowsell and O. M. Yaghi, *Microporous Mesoporous Mat.*, 2004, **73**, 3-14.
4. C. Janiak and J. K. Vieth, *New J. Chem.*, 2010, **34**, 2366-2388.
5. M. Eddaoudi, J. Kim, N. Rosi, D. Vodak, J. Wachter, M. O'Keeffe and O. M. Yaghi, *Science*, 2002, **295**, 469-472.
6. L. F. Ma, Y. Y. Wang, L. Y. Wang, D. H. Lu, S. R. Batten and J. G. Wang, *Cryst. Growth Des.*, 2009, **9**, 2036-2038.
7. B. L. Chen, S. C. Xiang and G. D. Qian, *Accounts Chem. Res.*, 2010, **43**, 1115-1124.
8. C. Janiak, *Dalton Trans.*, 2003, 2781-2804.
9. G. Scholz, F. Emmerling, M. Dreger and E. Kemnitz, *Zeitschrift Fur Anorganische Und Allgemeine Chemie*, 2013, **639**, 689-693.
10. S. R. Miller, E. Alvarez, L. Fradcourt, T. Devic, S. Wuttke, P. S. Wheatley, N. Steunou, C. Bonhomme, C. Gervais, D. Laurencin, R. E. Morris, A. Vimont, M. Daturi, P. Horcajada and C. Serre, *Chem. Commun.*, 2013, **49**, 7773-7775.
11. R. Babarao and J. W. Jiang, *Langmuir*, 2008, **24**, 6270-6278.
12. A. Thirumurugan and A. K. Cheetham, *Eur. J. Inorg. Chem.*, 2010, 3823-3828.
13. W. H. Bi, N. Leblanc, N. Mercier, P. Auban-Senzier and C. Pasquier, *Chem. Mat.*, 2009, **21**, 4099-4101.
14. V. Andre, A. Hardeman, I. Halasz, R. S. Stein, G. J. Jackson, D. G. Reid, M. J. Duer, C. Curfs, M. T. Duarte and T. Friscic, *Angew. Chem.-Int. Edit.*, 2011, **50**, 7858-7861.
15. P. C. Andrews, G. B. Deacon, C. M. Forsyth, P. C. Junk, I. Kumar and M. Maguire, *Angew. Chem.-Int. Edit.*, 2006, **45**, 5638-5642.
16. A. C. Wibowo, M. D. Smith and H. C. zur Loye, *Cryst. Growth Des.*, 2011, **11**, 4449-4457.
17. A. C. Wibowo, M. D. Smith, J. Yeon, P. S. Halasyamani and H. C. zur Loye, *Journal of Solid State Chemistry*, 2012, **195**, 94-100.
18. A. Thirumurugan, W. Li and A. K. Cheetham, *Dalton Trans.*, 2012, **41**, 4126-4134.
19. S. Busch, I. Stein and U. Ruschewitz, *Zeitschrift Fur Anorganische Und Allgemeine Chemie*, 2012, **638**, 2098-2101.
20. M. Feyand, M. Koppen, G. Friedrichs and N. Stock, *Chemistry-a European Journal*, 2013, **19**, 12537-12546.
21. S. R. Sushrutha and S. Natarajan, *Cryst. Growth Des.*, 2013, **13**, 1743-1751.
22. M. Klimakow, Klobes, P., Thunemann, A. F., Rademann, K., Emmerling, F., *Chem. Mat.*, 2010, **22**, 5216-5221.
23. M. Klimakow, P. Klobes, K. Rademann and F. Emmerling, *Micropor Mesopor Mat*, 2012, **154**, 113-118.
24. A. Delori, T. Friscic and W. Jones, *Crystengcomm*, 2012, **14**, 2350-2362.
25. T. Friscic, I. Halasz, V. Strukil, M. Eckert-Maksic and R. E. Dinnebier, *Croatica Chemica Acta*, 2012, **85**, 367-378.
26. S. Heiden, L. Trobs, K. J. Wenzel and F. Emmerling, *Crystengcomm*, 2012, **14**, 5128-5129.

27. V. Strukil, L. Fabian, D. G. Reid, M. J. Duer, G. J. Jackson, M. Eckert-Maksic and T. Friscic, *Chem. Commun.*, 2010, **46**, 9191-9193.
28. J. I. Langford and D. Louer, *Rep. Prog. Phys.*, 1996, **59**, 131-234.
29. P. C. Andrews, G. B. Deacon, W. R. Jackson, M. Maguire, N. M. Scott, B. W. Skelton and A. H. White, *J Chem Soc Dalton*, 2002, 4634-4638.
30. P. C. Andrews, G. B. Deacon, P. C. Junk, I. Kumar and M. Silberstein, *Dalton T*, 2006, 4852-4858.
31. T. Hatanpaa, M. Vehkamaki, M. Ritala and M. Leskela, *Dalton Trans.*, 2010, **39**, 3219-3226.
32. P. C. Andrews, V. L. Blair, R. L. Ferrero, P. C. Junk and I. Kumar, *Chem. Commun.*, 2013, **49**, 2870-2872.
33. L. M. Markham, L. C. Mayne, B. S. Hudson and M. Z. Zgierski, *J. Phys. Chem.*, 1993, **97**, 10319-10325.
34. T. V. 2.0, Bruker AXS, Karlsruhe (Germany), 2000.
35. J. Laugier and B. Bochu, Chekcell, 2001.
36. V. Favre-Nicolin and R. Cerny, *Journal of Applied Crystallography*, 2002, **35**, 734-743.
37. H. Riesemeier, K. Ecker, W. Gorner, B. R. Muller, M. Radtke and M. Krumrey, *X-Ray Spectrom*, 2005, **34**, 160-163.
38. W. Gorner, M. P. Hentschel, B. R. Muller, H. Riesemeier, M. Krumrey, G. Ulm, W. Diete, U. Klein and R. Frahm, *Nucl Instrum Meth A*, 2001, **467**, 703-706.
39. B. Ravel and M. Newville, *J. Synchrot. Radiat.*, 2005, **12**, 537-541.
40. J. J. Rehr, J. J. Kas, F. D. Vila, M. P. Prange and K. Jorissen, *Phys. Chem. Chem. Phys.*, 2010, **12**, 5503-5513.

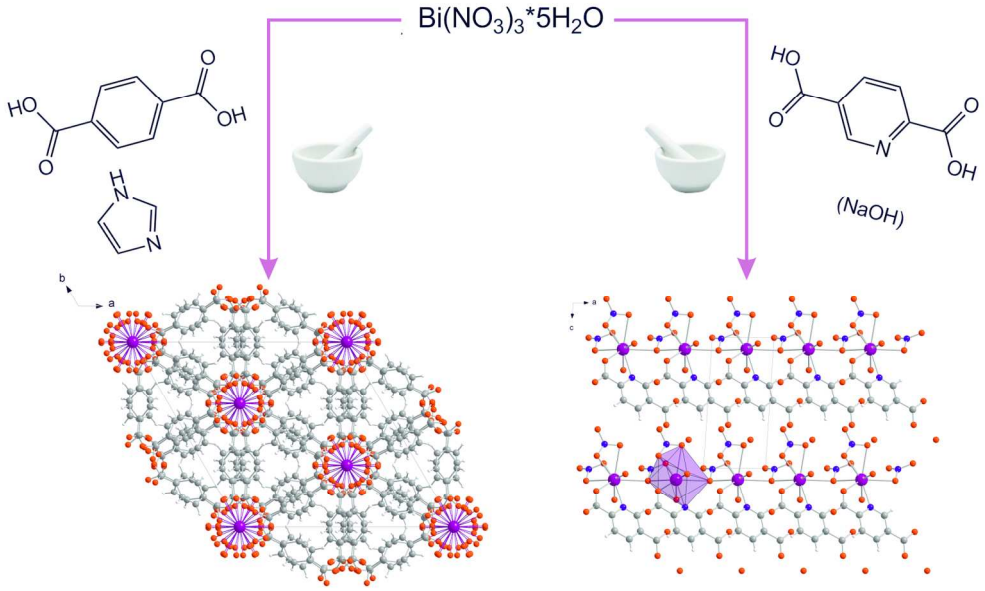

153x91mm (300 x 300 DPI)